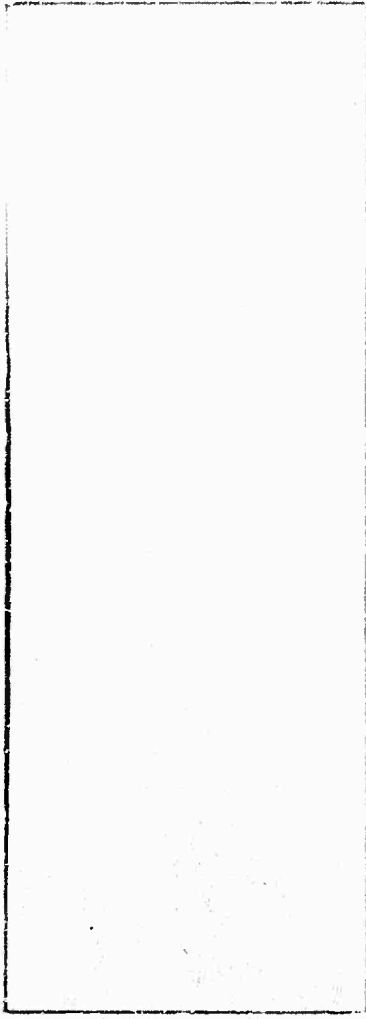


AD626816



PHILCO.
A SUBSIDIARY OF *Ford Motor Company.*
AERONUTRONIC DIVISION

PROPERTY
OF
GODDARD SPACE FLIGHT CENTER

LIBRARY D.C.
JAN 18 1956
PROPERTY OF THE
NASA

83980

DISCLAIMER NOTICE

**THIS DOCUMENT IS THE BEST
QUALITY AVAILABLE.
COPY FURNISHED CONTAINED
A SIGNIFICANT NUMBER OF
PAGES WHICH DO NOT
REPRODUCE LEGIBLY.**

Under Contract: NOnr 3560(00)
ARPA Order No. 273/11-7-63


6 August 1965

SCIENTIFIC REPORT

ABSORPTION BY CO₂ BETWEEN 8000 AND 10,000 cm⁻¹
(1 - 1.25 Micron Region)

Prepared for: Advanced Research Projects Agency
Washington 25, D. C.

Prepared by: Darrell E. Burch
David A. Gryvnak
Richard R. Patty

Approved: 
M. H. Johnson, Director
Physics Laboratory

"This material is the result of tax-supported research and as such may be freely reprinted with the customary crediting of the source."

Handwritten signature

AERONUTRONIC
DIVISION OF PHILCO CORPORATION
A SUBSIDIARY OF Ford Motor Company,
FORD ROAD, NEWPORT BEACH, CALIF.

ABSTRACT

The absorption by CO_2 in the 9300 to 9650 cm^{-1} region (1.0 μ) and 8000 to 8325 cm^{-1} region (1.2 μ) have been studied. Spectra were obtained for four samples of CO_2 in the 1.0 μ region at a pressure of 2.5 atmospheres and path lengths up to 932 meters. Spectra were obtained for ten samples of CO_2 in the 1.2 μ region at pressures as high as 15 atmospheres for path lengths up to 32.9 meters and pressures as high as 2.50 atmospheres for path lengths up to 933 meters. The strengths of the important bands and the half-widths of several lines have been measured. Tables of transmittance versus wavenumber are included for both regions as well as photographs of most of the spectra. Also presented are tables of the integrated absorbance $\int_{\nu}^{\nu} A(\nu) d\nu$ versus ν for both regions.

TABLE OF CONTENTS

SECTION		PAGE
1	INTRODUCTION AND SUMMARY.	1-1
2	EXPERIMENTAL METHODS AND NOTATION	2-1
	2.1 Apparatus and Procedure.	2-1
	2.2 Definitions, Symbols and Notations	2-2
3	DISCUSSION OF ABSORPTION BANDS.	3-1
3.1	Identification and Features of the Absorption Bands	3-1
	Table 3-1, Positions and Strengths of	
	Absorption Bands.	3-2
	Figure 3-1, Transmission Spectra of the	
	9300-9650 cm^{-1} Region	3-4
	Figure 3-2, Transmission Spectra of the	
	8000-8350 cm^{-1} Region	3-5
	Figure 3-3, Transmission Spectra of the	
	8000-8350 cm^{-1} Region	3-6
	Table 3-2, Sample Parameters	3-7
3.2	Band Strengths	3-8
3.3	Half-Widths of Absorption Lines.	3-11
	Figure 3-4, Half-Widths of Self-Broadened	
	CO_2 Lines at 1 Atm. Pressure	3-13
4	TABLES OF TRANSMITTANCE	4-1
	Table 4-1, Table of Transmittances (9340-9660 cm^{-1})	4-2
	Table 4-2, Table of Transmittances (8030-8340 cm^{-1})	4-3
5	TABLES OF INTEGRATED ABSORPTANCE.	5-1
	Table 5-1, Table of Integrated Absorptance	
	(9430-9660 cm^{-1})	5-2
	Table 5-2, Table of Integrated Absorptance	
	(8030-8340 cm^{-1})	5-3
6	REFERENCES.	6-1

(This page is intentionally left blank.)

SECTION 1

INTRODUCTION AND SUMMARY

Most of the important absorption bands of CO_2 in the region between 8000 and 10,000 cm^{-1} have been observed by Herzberg and Herzberg.¹ These workers contained their samples in a multiple-pass absorption cell which was capable of very long paths and obtained their spectra photographically. They measured the positions of many of the lines and the centers of several of the bands with very good accuracy; but very little can be learned about the strengths or widths of the absorption lines from their data.

The present investigation was undertaken to obtain spectra of samples covering a wide range of pressures and path lengths. From the results included in this report, the strengths of nearly all of the lines of any importance and the widths of several of them can be determined. From this information, one can, at least in principle, calculate the transmission over an extremely wide variation of paths, including those in which the pressure, temperature and the mixing ratio of CO_2 with other gases might vary.

The band near 9500 cm^{-1} is of particular importance at the present time in the interpretation of spectra of the atmospheres of Mars and Venus. It occurs in a region free of absorption lines of other atmospheric gases; therefore, spectra of the planetary atmospheres can be obtained from the earth's surface. This band is so weak that its integrated absorptance in the Martian atmosphere should be very nearly independent of the pressure of the gas. Thus, by comparing the planetary spectra with laboratory spectra such as some of those presented below, one should be able to determine the amount of CO_2 in the Martian atmosphere.

Once the amount of CO₂ is known, the pressure can be determined by investigating other bands in which the absorption is a function of both the amount of CO₂ and the total pressure.

Spectra of several samples are shown in Section 3 with a discussion of the various features of the bands. The strengths, or absolute intensities, of the important bands have been determined, and the half-widths of several of the lines have been measured. Section 4 includes a table of transmittance versus wavenumber for 14 different samples studied. Section 5 contains tables of the integrated absorbance $\int A(\nu)d\nu$ for the same samples; from this table the integrated absorbance over virtually any region of interest in the bands can be determined.

SECTION 2

EXPERIMENTAL METHODS AND NOTATION

2.1 APPARATUS AND PROCEDURE

Samples of CO_2 were contained in two different absorption cells which have been described previously.² The longer cell has a base length of approximately 30 meters and was used at as many as 32 passes, giving a total path length of 933 meters. It is approximately 0.9 meters in diameter and can be evacuated to less than one micron of Hg or pressurized to as much as 2.5 atmospheres. The shorter cell has a base length of approximately 1 meter and was used at as many as 32 passes. It can be evacuated or pressurized to as much as 15 atmospheres.

The CO_2 was drawn from the vapor in a dewar which contained both liquid and vapor at a pressure of about 300 psig and a temperature of approximately -20°C . We found that samples obtained in this manner contained fewer impurities, particularly H_2O , than samples taken from commercial cylinders at room temperature. A spectrum published previously by us shows a small amount of absorption in the region between approximately 9530 and 9560 cm^{-1} which is apparently due to an impurity since the absorption does not appear in more recent spectra of samples obtained in the manner described above.

The spectra were obtained with an Ebert type spectrometer whose main mirror has a 75 cm focal length. The region from 9000 to $10,000\text{ cm}^{-1}$ was scanned with a grating having 1200 lines/mm and blazed at $0.8\ \mu$. It was used in the first order and a Tiffen glass filter eliminated overlapping orders of shorter wavelengths. The region between 8000 and 9000 cm^{-1} was studied with a grating having 300 lines/mm and blazed at $3.2\ \mu$. Overlapping orders were eliminated in this region by the use of a silico. window. Both gratings have a ruled area of $64 \times 64\text{ mm}$.

A PbS cell cooled with liquid nitrogen was used as the detector. It was not necessary to cool the detector below dry ice temperature for operation in this wavelength region, but the dewar on the detector was designed to hold liquid nitrogen for use at longer wavelengths. Cooling by liquid nitrogen was, therefore, more convenient and was used since the signal-to-noise ratio was approximately the same at both temperatures. A considerably better signal-to-noise ratio (S/N) could probably be achieved in the region between 9000 and 10,000 cm^{-1} with a photomultiplier detector. However, the extra sensitivity of the photomultiplier was not required in order to obtain spectra from which the strengths of the bands in this region can be determined. The S/N in the 8000 - 9000 cm^{-1} region was enough higher than in the higher wavenumber region that we could conveniently work with a smaller spectral slitwidth. Most of the spectra in the lower wavenumber region were obtained with sufficiently good spectral resolution that many of the lines could be resolved. However, in the higher wavenumber region the slits were opened until a desirable S/N was obtained.

Wavenumber calibration was obtained for each spectrum from the positions of the absorption lines and band centers designated in Figures 3-1 and 3-2, most of which are from Herzberg and Herzberg.¹

The raw spectra were replotted and digitized by the use of apparatus described in Appendix C of reference 2. A computer program was then used to calculate values of transmittance and integrated absorbance which are shown in Sections 4 and 5.

2.2 DEFINITIONS, SYMBOLS AND NOTATIONS

L is the geometrical path length of the radiation as it passes through a sample, p is the pressure of the CO_2 which is measured in atmospheres unless otherwise specified, and u is the absorber thickness given by

$$u = W p L \frac{273}{296} \text{ (atm cm}_{\text{STP}}^{\text{)}}. \quad (2-1)$$

W is a factor that accounts for the Van der Waals' forces which cause CO_2 to deviate from a perfect gas at some of the pressures used in this investigation. It is given adequately for our purposes by

$$W = 1.00 + 0.0047 p. \quad (2-2)$$

The quantity 273/296 accounts for the difference in density between standard temperature (273°K) and room temperature (296°K) at which all of the measurements were made. The absorber thickness given by Equation (2-1) is then equivalent to the thickness of a CO_2 sample at 1 atmosphere pressure and 273°K having the same number of molecules per unit area as the sample being described.

Although this investigation deals only with samples of pure CO₂, it is frequently desirable to relate the pressures to an equivalent pressure P_e of a dilute mixture of CO₂ in N₂. This is necessary when dealing with paths through the earth's atmosphere in which the partial pressure of CO₂ is small compared to that of N₂. Burch, Gryvnak and Williams⁴ have found that throughout most of the spectrum an equivalent pressure given by

$$P_e = 1.3 p + (P - p) \quad (2-3)$$

can be used where P is the total pressure due to both gases. It is noted that the equivalent pressure approaches the total pressure for a very dilute mixture of CO₂ in N₂. The factor 1.3 relates the self-broadening ability of CO₂ to the broadening ability of CO₂ lines by N₂. It is valid in regions where most of the absorption is due to lines whose centers are within a few cm⁻¹; but it is not valid in regions such as on the high wavenumber side of the ν₃ and 3ν₃ bands where the absorption is due to the extreme wings of lines whose centers are several cm⁻¹ away. Variations in the shapes of the extreme wings of CO₂ absorption lines give rise to the difference in the relative broadening abilities. The line shapes of different broadening gases will be discussed in a report⁵ to be published by us in the near future.

Since the simple classical theory predicts that the half-width of a line is proportional to the density of molecules, Equation (2-3) should probably be modified to account for the non-linearity between pressure and density at higher pressures. The modification can be made in the following way:

$$P_e = 1.3 W p + (P - p). \quad (2-3')$$

T(v) is the observed transmittance and A(v) ≡ 1 - T(v) is the observed absorbance. T'(v) and A'(v) are the transmittance and absorbance, respectively, which would be observed with an instrument having infinite resolving power. T'(v) is related to the absorption coefficient K(v) by

$$T'(v) = \exp \left[-u K(v) \right] \quad \text{or} \quad -\ln T'(v) = u K(v). \quad (2-4)$$

α is the half-width of an absorption line and is expressed in cm⁻¹. S_v is the band strength, or band intensity, and is related to the absorption coefficient due to the band of interest by

$$S_v = \int K(v) dv. \quad (2-5)$$

(This page is intentionally left blank.)

SECTION 3

DISCUSSION OF ABSORPTION BANDS

3.1 IDENTIFICATION AND FEATURES OF THE ABSORPTION BANDS

All of the CO_2 bands which one might expect to produce appreciable absorption in the region from 8000 to $10,000 \text{ cm}^{-1}$ are listed in Table 3-1. The positions of the band centers measured by Herzberg and Herzberg¹ and by Courtoy⁶ are listed. Centers of the other bands were calculated from energy levels tabulated by Stull, Wyatt and Plass.⁷ In the notation for the transitions, the lower level is omitted when it is 00^0_0 . The strengths of the different portions of the bands are described in Section 3.2.

The bands occur in two groups, one between 9300 and 5650 cm^{-1} and the other between 8000 and 8325 cm^{-1} . All of the bands arise from transitions in which there is a change of three (3) in ν_3 , the quantum number associated with ν_3 . Since, for CO_2 , $\nu_1 = 2\nu_2$, the bands arising from transitions from the ground state to 20^0_3 , 1^0_03 , and 04^0_0 occur close to each other. These bands, along with their associated difference bands, occur in the region from 9300 to 9650 cm^{-1} . The changes in each of the quantum numbers are the same for the difference bands as for the combination bands, but the difference bands arise from transitions from the 01^1_0 state.

Because of anharmonicity, a difference band usually occurs at a slightly lower wavenumber than its associated combination or fundamental band. However, the displacement of the difference band varies from one band to another, depending on the Fermi resonance.

TABLE 3-1
POSITIONS AND STRENGTHS OF ABSORPTION BANDS

Band Center cm ⁻¹	Transition ^a	Portion	Strength atm ⁻¹ cm ⁻¹	Strength SFP cm ⁻¹
9631.38	HH ^b 20 ⁰ 3	R-Branch P-Branch Entire Band	1.4 1.25 2.6	+ 0.13 x 10 ⁻⁵ + 0.14 x 10 ⁻⁵ - 0.25 x 10 ⁻⁵
9629.6	SWP 21 ¹³ +01 ¹⁰	Entire Band ^c	2.0	x 10 ⁻⁶
9517.00	HH 12 ⁰ 3	K-Branch P-Branch Entire Band	3.40 3.23 6.63	+ 0.2 x 10 ⁻⁵ + 0.5 x 10 ⁻⁵ - 0.7 x 10 ⁻⁵
9478.2	SWP 13 ¹³ +01 ¹⁰	Entire Band ^c	5.2	x 10 ⁻⁶
9389.02	HH 04 ⁰ 3	R-Branch P-Branch Entire Band	6.5 5.5 12.5	+ 0.7 x 10 ⁻⁶ + 1 x 10 ⁻⁶ - 1.5 x 10 ⁻⁶
9320.1	SWP 05 ¹³ +01 ¹⁰		not measurable	
8294.01	HH 10 ⁰ 3	R-Branch P-Branch Entire Band	8.4 8.6 17.0	+ 0.6 x 10 ⁻⁴ + 0.6 x 10 ⁻⁴ - 1.0 x 10 ⁻⁴
8276.83	HH 11 ¹³ +01 ¹⁰	Entire Band ^c	1.5	x 10 ⁻⁴
8243.2	SWP 20 ⁰ 3+10 ⁰⁰		Not observable	
8231.6	SWP 12 ⁰ 3+02 ⁰⁰		Not observable	
8220.0	SWP 10 ⁰ 3 (C ¹² O ¹⁶ O ¹⁸)		Not observable	
8192.62	HH 02 ⁰ 3	R-Branch P-Branch Entire Band	6.0 5.8 11.8	+ 0.5 x 10 ⁻⁴ + 0.5 x 10 ⁻⁴ - 0.9 x 10 ⁻⁴
8135.95	HK (3 ¹³ +01 ¹⁰)	Entire Band	1.0	+ 0.2 x 10 ⁻⁴
8128.8	SWP 12 ⁰ 3+10 ⁰⁰		Not observable	
8119.7	SWP 02 ⁰ 3 (C ¹² O ¹⁶ O ¹⁸)		Not observable	
8103.7	SWP 04 ⁰ 3+02 ⁰⁰		Not observable	
8089.01	C 10 ⁰ 3 (C ¹³ O ¹⁶)	Entire Band	2.5	+ 1 x 10 ⁻⁵

^aTransitions for isotope C¹²O¹⁶ unless otherwise specified.

^bAuthority for position of band center. HH and C refer to Herzberg and Herzberg¹ and to Courtoy,⁶ respectively. SWP denotes that band centers were calculated from energy levels tabulated by Stull, Wyatt and Plass.⁷

^cStrengths of difference bands were calculated from combined strengths of difference band and associated combination band by use of Equation (3-3).

Spectra of the $9390 - 9650 \text{ cm}^{-1}$ region are shown in Figure 3-1 with the positions of the band centers indicated in the lower panel. The curve in the lower panel is a replot of the original spectrum of the largest sample studied in this investigation; it was obtained with the spectral slitwidth sufficiently wide that the structure of the band was lost. The upper panel shows a photograph of an original spectrum of a different sample obtained with considerably narrower slits. This spectrum is rather noisy, but the structure in the P-branch of the three stronger bands is apparent. The magnitude of the noise in the spectrum can be seen in the region above about 9650 cm^{-1} , as well as in the regions just above the heads of the other bands. All the spectra used in the analysis were obtained with wider slits in order to reduce the noise to less than 2 or 3% of the signal.

The 20^0_3 and $21^1_3-01^1_0$ bands are not resolved and appear as a single band since their centers are separated by only about 1.8 cm^{-1} . The $13^1_3-01^1_0$ band overlaps the P-branch of the 12^0_3 band, with evidence of the head of the former at about 9495 cm^{-1} . The 04^0_3 band is weaker than the other two; its associated difference band ($05^1_3-01^1_0$ band) is very weak and is not included in the spectrum shown. Only a hint of absorption could be observed on the spectrum of our largest sample in the region where this band should occur.

The 10^0_3 and 02^0_3 bands are separated by approximately 100 cm^{-1} and occur in the region between 8000 and 8325 cm^{-1} along with their associated difference bands. Figures 3-2 and 3-3 show spectra of several different samples obtained in this region. The numbers enclosed in rectangles are the sample numbers listed in Table 3-2. The positions of the centers of the more important bands are indicated in the lower panel of Figure 3-2. The center of the $11^1_3-01^1_0$ band occurs in the P-branch of the 10^0_3 band with the head of the difference band near the center of the 10^0_3 band. The effect of the difference band on the absorption near 8280 cm^{-1} can be seen easily in the spectrum of Sample 8. The $03^1_3-01^1_0$ band also occurs in the P-branch of its associated combination band (02^0_3); its presence is more apparent since the band head occurs further from the center of the stronger band.

The difference bands due to transitions from the 02^0_0 and 10^0_0 states could probably be seen in the spectra of our largest samples if they were not overlapped by the lines of stronger bands. Resolution considerably better than that employed in this investigation would be required in order to observe the lines of these bands between the much stronger ones.

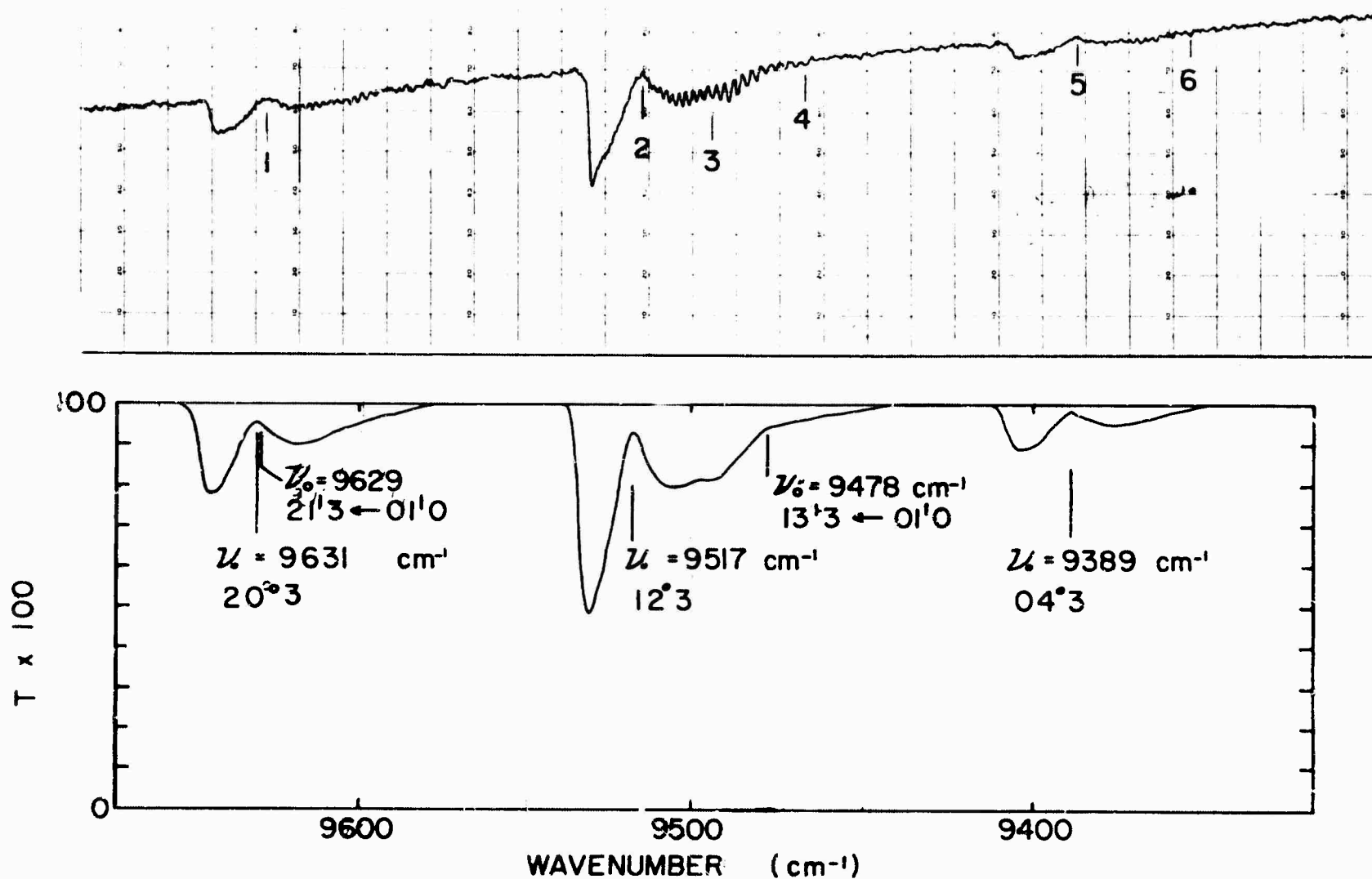


FIGURE 3-1 TRANSMISSION SPECTRA OF THE 9300 - 9650 cm^{-1} REGION.

The upper curve is a photograph of an original spectrum obtained with a slitwidth of about 1.3 cm^{-1} for a sample of pure CO_2 with $p = 2.50 \text{ atm}$ and $u = 10.9 \times 10^4 \text{ atm cm}_{\text{STP}}$. The lower curve was replotted from a spectrum of Sample 4 ($p = 2.50 \text{ atm}$, $u = 21.7 \times 10^4 \text{ atm cm}_{\text{STP}}$) with a spectral slitwidth of 3.8 cm^{-1} . The wavenumbers of the centers of the bands are indicated. Note that the wavenumber scales are not the same in both panels. Wavenumbers of the points indicated in the upper panel are: 1, 9631.4 cm^{-1} ; 2, 9517.00 cm^{-1} ; 3, 9495.33 cm^{-1} ; 4, 9467.50 cm^{-1} ; 5, 9389.02 cm^{-1} ; 6, 9356.23 cm^{-1} . These points were used for wavenumber calibration.

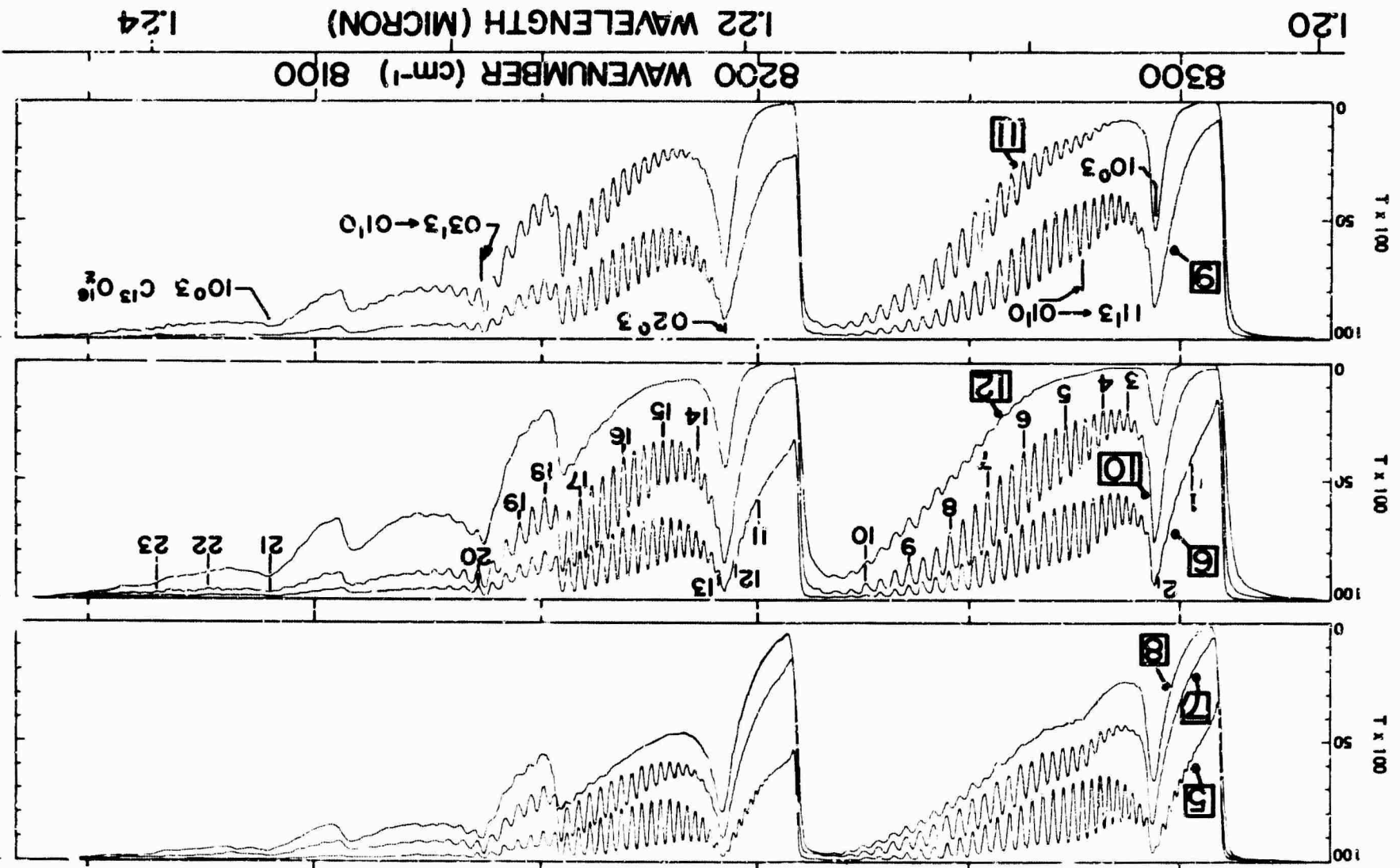


FIGURE 3-2 TRANSMISSION SPECTRA OF THE 8000 - 8350 cm⁻¹ REGION.

The wavenumbers of the centers of the bands are indicated in the lower panel. Numbers enclosed in rectangles are sample numbers (See Table 3-2). Wavenumbers of the points indicated in the middle panel are: 1, 8302.4 cm⁻¹; 2, 8294.8 cm⁻¹; 3, 8287.2 cm⁻¹; 4, 8281.4 cm⁻¹; 5, 8272.5 cm⁻¹; 6, 8262.4 cm⁻¹; 7, 8254.1 cm⁻¹; 8, 8245.1 cm⁻¹; 9, 8235.5 cm⁻¹; 10, 8225.2 cm⁻¹; 11, 8200.0 cm⁻¹; 12, 8194.8 cm⁻¹; 13, 8191.0 cm⁻¹; 14, 8185.9 cm⁻¹; 15, 8178.0 cm⁻¹; 16, 8169.1 cm⁻¹; 17, 8159.0 cm⁻¹; 18, 8150.7 cm⁻¹; 19, 8144.9 cm⁻¹; 20, 8135.6 cm⁻¹; 21, 8089.6 cm⁻¹; 22, 8076.4 cm⁻¹; 23, 8065.2 cm⁻¹. These points were used for wavenumber calibration.

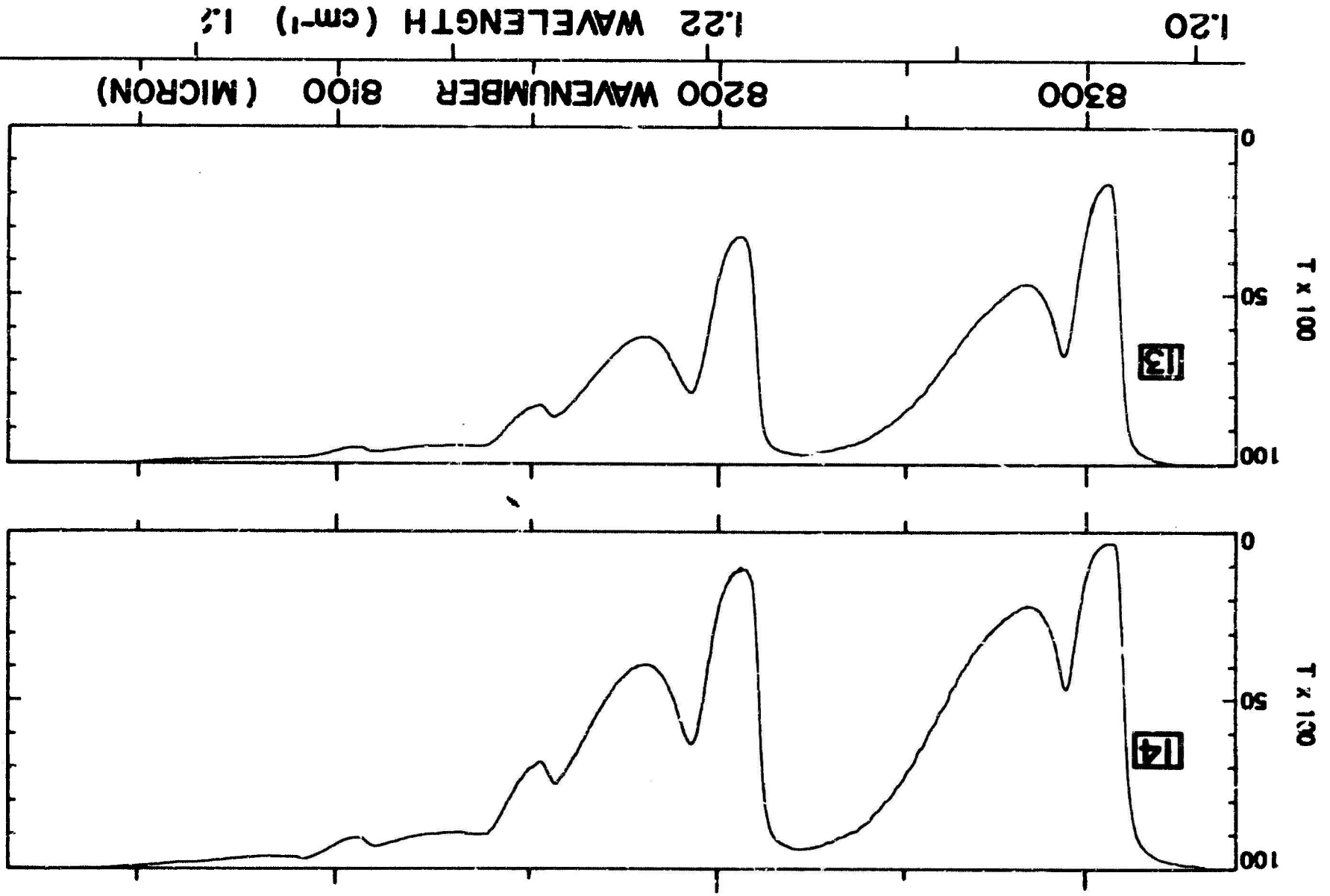


FIGURE 3-3 TRANSMISSION SPECTRA OF THE 8000 - 8350 cm^{-1} REGION.

The curves show spectra of samples 13 and 14 obtained at a pressure of 14.6 atm in order to smooth out the structure. These points were used for wavenumber calibration.

TABLE 3-2

SAMPLE PARAMETERS

Sample No.	P torr	P atm	u atm cm ³ STP	L Meters	Spectral Slit width (cm ⁻¹)	Figure in which spectrum is shown
1	1900	2.50	5.51 x 10 ⁴	237	2.5	Not shown
2	1900	2.50	10.9 x 10 ⁴	469	2.5	Not shown
3	1900	2.50	16.3 x 10 ⁴	701	3.8	Not shown
4	1900	2.50	21.7 x 10 ⁴	933	3.8	3-1
5	758	0.997	1.11 x 10 ⁴	121	1.2	3-2
6	758	0.997	2.18 x 10 ⁴	237	1.5	3-2
7	758	0.997	4.32 x 10 ⁴	469	1.9	3-2
8	758	0.997	8.60 x 10 ⁴	933	2.8	3-2
9	1920	2.53	2.83 x 10 ⁴	121	1.5	3-2
10	1920	2.53	5.57 x 10 ⁴	237	1.5	3-2
11	1920	2.53	11.0 x 10 ⁴	469	1.9	3-2
12	1920	2.53	21.9 x 10 ⁴	933	2.8	3-2
13	11,100	14.6	2.38 x 10 ⁴	16.5	1.1	3-3
14	11,100	14.6	4.73 x 10 ⁴	32.9	1.1	3-3

The 10⁰3 band of C¹³O₂¹⁶ can be seen with its center at 8089.0 cm⁻¹. It was identified as 02⁰3 by Herzberg and Herzberg¹ and later identified as 10⁰3 by Courtoy.⁷ Stull, Wyatt and Plass⁷ give 8089.0 cm⁻¹ for the band center of 10⁰3 and 7981.1 cm⁻¹ for 02⁰3. The latter band is very weak and will be discussed in a future report covering the region between 7100 and 8000 cm⁻¹. The 10⁰3 and 02⁰3 bands of C¹²O₁₆¹⁸ should be sufficiently strong to be observed in the spectrum of our largest samples if they were not overlapped by lines of the stronger bands. Like the difference bands mentioned above, lines of these isotopic bands could probably be seen with better resolution. No attempt was made to change the relative abundances of the isotopes in our samples. It is probably safe to assume that they occur in their natural abundances.

It is noted that all of the bands in this region have a rather sharp band head on the high wavenumber side of the R-branch, a feature which is typical of CO₂ bands having a change in the quantum number ν_3 associated with ν_3 . The heads of the bands included in this report occur near $J = 44$ in the R-branch.

3.2 BAND STRENGTHS

The strength, or intensity, of an absorption band is given by

$$S_v = \int K(\nu) d\nu, \quad (2-5)$$

where the integration is performed over all ν for which there is appreciable absorption. $K(\nu)$, the absorption coefficient, is defined by Equation (2-4).

Of course, if more than one band contributes to the absorption at a given wavenumber, $K(\nu)$ used in Equation (2-5) must include only the portion due to the band whose strength is being determined. The methods used to estimate the contributions of each band in overlapping regions are described below.

The strengths of the bands included in this report are essentially independent of pressure over the range of pressures used. However, as the pressure is increased, the lines are broadened until at 14.6 atm, the maximum pressure used, the half-widths are of the order of 1.3 cm^{-1} . This is less than the spectral slitwidth used in obtaining spectra of Samples 13 and 14 (Figure 3-3). Consequently, the observed transmittance $T(\nu)$ is very nearly the true transmittance $T'(\nu)$. By combining Equations (2-4) and (2-5), we see that we can determine the band strengths from the spectra by use of the following equation.

$$S_v = -\frac{1}{u} \int \ln T(\nu) d\nu. \quad (3-1)$$

Equation (3-1) was used to determine the strengths of all the bands in the 8000 - 8325 cm^{-1} region from Samples 13 and 14, except for the 1003 band of Cl_2O . It was not possible to use samples in the shorter absorption cell with sufficiently large absorber thickness to produce more than a few percent absorbance by this band or by the bands in the 9300 - 9650 cm^{-1} region. Therefore, the strengths of these bands were determined from spectra of samples contained in the longer absorption cell whose maximum pressure is 2.5 atmospheres. At this pressure $T'(\nu)$ may be quite different from $T(\nu)$; but Equation (3-1) can still be used, provided $A(\nu) \approx 1 - T(\nu)$ is not too large. A more detailed discussion of the limitations on (3-1) when dealing with samples at relatively low pressures is given in Reference 8.

For Σ - Σ bands (quantum number $\ell = 0$) of CO_2 , the strength S_m of a given line within a band is related to the band strength S_v by

$$S_m = S_v \left| m \right| \exp \left[-\frac{B'' m(m-1)}{k\theta} \right] / Q_r. \quad (3-2)$$

$m = J + 1$ for the R-branch and $-J$ for the P-branch. B'' is the rotational constant of the lower state, k is Boltzmann's constant, θ is the temperature, and Q_r is the rotational partition function. The Q-branch is missing in $\Sigma \rightarrow \Sigma$ bands, and contains only about one percent of the strength of $\Pi \rightarrow \Pi$ bands ($\mathcal{L} = 1$ as in $21^{13}+01^{10}$). Equation (3-2) also gives the strengths of lines in the P- and R-branches of $\Pi \rightarrow \Pi$ bands. Gray and Selvidge⁹ have tabulated values of partition functions and relative line strengths for different types of CO_2 bands at several temperatures.

According to quantum theory,¹⁰ the relative strength of the difference band $21^{13}+01^{10}$ to its associated summation band 20^{03} is given by

$$\frac{S_V(21^{13}+01^{10})}{S_V(20^{03})} = 2 \exp(-hc 667.4/k\theta) \quad (3-3)$$

$$= 0.078 \text{ for } \theta = 296^\circ\text{K.}$$

h is Planck's constant, c is the speed of light and the factor 2 arises from the double degeneracy of the 01^{10} state. 667.4 cm^{-1} is the difference between the energy levels 01^{10} and 00^{00} .

Equation (3-3) also relates the strength of any difference band to its associated summation or fundamental band if the proper degeneracy factor is used and 667.4 is replaced by the difference between the energy level 00^{00} and the lower level for the difference band.

The strengths of all the bands of significance in the region are given in Table 3-1. From Equations (3-1) and (2-1), we see that the units of band strength are $\text{atm}^{-1} \text{cm}^{-1} \text{cm}^{-1}_{\text{STP}}$, with the STP referring to the absorber thickness and not to the temperature at which the measurement was made.

Since the 20^{03} and $21^{13}+01^{10}$ bands are not separated in our spectra, their strengths were calculated from their combined strengths by the use of Equation (3-3). The R- and P-branches could be measured separately, and their relative strengths are in good agreement with what we obtain by summing the strengths of the lines in each branch as given by (3-2). The summation gives 52% for the R-branch and 48% for the P-branch.

The R-branch of the 12^{03} band is isolated from other bands and could be measured separately. But the P-branch is overlapped by the $13^{13}+01^{10}$ band, making it necessary to use Equation (3-3) to determine their strengths.

The 04^{03} band is displaced from its associated difference band ($05^{13}+01^{10}$) and could be measured directly. There was only a hint of absorption in our original spectra in the region where $05^{13}+01^{10}$ should appear. Therefore,

its strength could not be measured; it could, of course, be calculated from the strength of the 04^0_3 band.

No values of uncertainty are presented for the strengths of the difference bands since they would depend on the uncertainties of the associated combination bands and on the error in the theoretical relationship given by Equation (3-2). In some cases the uncertainty of an entire band is slightly less than the sum of the two branches since it is not possible to divide the spectrum exactly to determine the contributions of each branch.

The R-branches of the 10^0_3 and 02^0_3 bands of $C^{12}O_2^{16}$ are relatively free of overlapping lines and were measured separately. Strengths of the $11^{13}3\text{-}01^{10}$ band and the P-branch of the 10^0_3 band were determined from Equation (3-3) in the same manner as the bands discussed above.

Although a portion of the P-branch of the 02^0_3 band is overlapped by the $03^{13}3\text{-}01^{10}$ band, lines P2 to P34 are isolated. By summing the strengths of lines P2 to P34 as given by Equation (3-2), we found that these lines comprise 90.7% of the strength of the entire P-branch. Therefore, the strength of the P-branch was determined from $\int K(\nu)d\nu/.907$ over the region from the band center to a point midway between P34 and P36. Allowance was made for the contribution of the wings of these lines which would occur outside the interval. The correction was calculated by assuming the lines have a Lorentz line shape and a half-width of 1.3 cm^{-1} . (This value of half-width is based on results shown in Section 3.3.) It was not necessary to calculate the correction very accurately since it amounted to only a couple percent of the strength of the P-branch.

The strength of the $03^{13}3\text{-}01^{10}$ band was then determined from $\int K(\nu)d\nu$ over the interval covered by the band and subtracting the portion due to the P-branch of the 02^0_3 band. It was also necessary to account for the overlapping 10^0_3 band of $C^{13}O_2^{16}$. By this method we were able to obtain values for the strengths of a combination band and its associated difference band with only a rather small correction based on a theoretical relationship. We see that the relative strengths are $1.0 \times 10^{-4}/11.8 \times 10^{-4} = 0.085$, which agrees, within experimental error, with 0.078 given by Equation (3-3).

The percent of uncertainty for the strength of the 10^0_3 band of $C^{13}O_2^{16}$ is large because of the sizeable corrections which had to be made for the overlapping bands. The strength given for this band is based on samples in which the relative abundances of the various isotopes were not intentionally altered. If we assume that the sample contains 98.9% C^{12} and 1.1% C^{13} , we would expect that, at least in the first approximation, the strengths of the bands of the two isotopes would be in the same ratio. This is seen to be true within experimental error. The ratio of strengths is $2.5 \times 10^{-5}/17.0 \times 10^{-4} = 0.015$, with approximately 40% uncertainty; and the ratio of abundances = 0.011.

3.3 HALF-WIDTHS OF ABSORPTION LINES

The shape of a collision-broadened CO_2 absorption line within a few cm^{-1} of its center, can usually be represented by the Lorentz line shape equation,^{5,11}

$$k(\nu) = \frac{S_m}{\pi} \frac{\alpha}{(\nu - \nu_0)^2 + \alpha^2} \quad (3-4)$$

$k(\nu)$ is the absorption coefficient of the single line; S_m is its strength, ν_0 is the line center, and α is the half-width. α is proportional to pressure while S_m and ν_0 are constant.

Ladenberg and Reiche¹² have shown that the integrated absorbance $\int A(\nu) d\nu$ of a single line having the Lorentz shape is given by

$$\int A(\nu) d\nu = 2\pi\alpha \mathcal{F}(x), \quad (3-5)$$

where $x = S_m u / 2\pi\alpha$, and

$$\mathcal{F}(x) = x e^{-x} \left[J_0(\lambda x) - \lambda J_1(\lambda x) \right]. \quad (3-6)$$

$J_0(\lambda x)$ and $J_1(\lambda x)$ are the Bessel functions of order 0 and 1, respectively.

Although Equation (3-6) is a rather involved expression, two well-known approximations can be readily used for single lines under certain conditions:

$$\int A(\nu) d\nu = S_m u, \quad \text{for small } x \quad (\text{weak lines}) \quad (3-7)$$

and

$$\int A(\nu) d\nu = 2 (S_m u \alpha)^{1/2} \quad \text{for large } x \quad (\text{strong lines}). \quad (3-8)$$

It is noted that Equations (3-7) and (3-1) are equivalent for small $A(\nu)$. Values of $\mathcal{F}(x)$ for intermediate x have been tabulated by Kaplan and Eggers.¹³

It is apparent from Equation (3-8) that α can be determined from a measurement of $\int A(\nu) d\nu$ under the proper conditions if S_m is known. $\int A(\nu) d\nu$ is seen to be independent of α for small x and proportional to $\alpha^{1/2}$ for large x . The dependence is less than square root for intermediate x ; and even if the conditions for Equation (3-8) are not fulfilled, α can still be determined by use of the exact expression given by Equation (3-5), provided x is sufficiently large that there is a sizeable dependence on α .

Lines P2 to P32 of the $O_2^{O_3}$ band are isolated from other lines of any significance; therefore, it was possible to measure $\int A(\nu)d\nu$ for them. Values of S_m were obtained from the band strength given in Table 3-1 by the use of Equation (3-2); and values of $\int A(\nu)d\nu$ were taken from Table 5-2 for each line. The absorber thickness u for Samples 6, 7 and 8 is great enough that x is sufficiently large for a near square-root dependence of $\int A(\nu)d\nu$ on α .

We assumed α^0 (α at a pressure of 1 atm) to be 0.09 cm^{-1} and used Equation (3-5) along with the tabulated values of $\int A(\nu)d\nu$ to calculate $\int A(\nu)d\nu$ for these samples. The calculated values of $\int A(\nu)d\nu$ were then compared with the observed values; and, by a reiterative process, more accurate values of α^0 were obtained.

In making the calculations, we accounted for slight overlapping of the lines which causes the integrated absorbance of a region containing several lines to be less than the sum of the individual contributions we would expect without overlapping. The maximum correction to the calculated $\int A(\nu)d\nu$ for overlapping was only about 5 percent. Results of a recent theoretical article by Plass¹⁴ were used to calculate the overlapping correction factor.

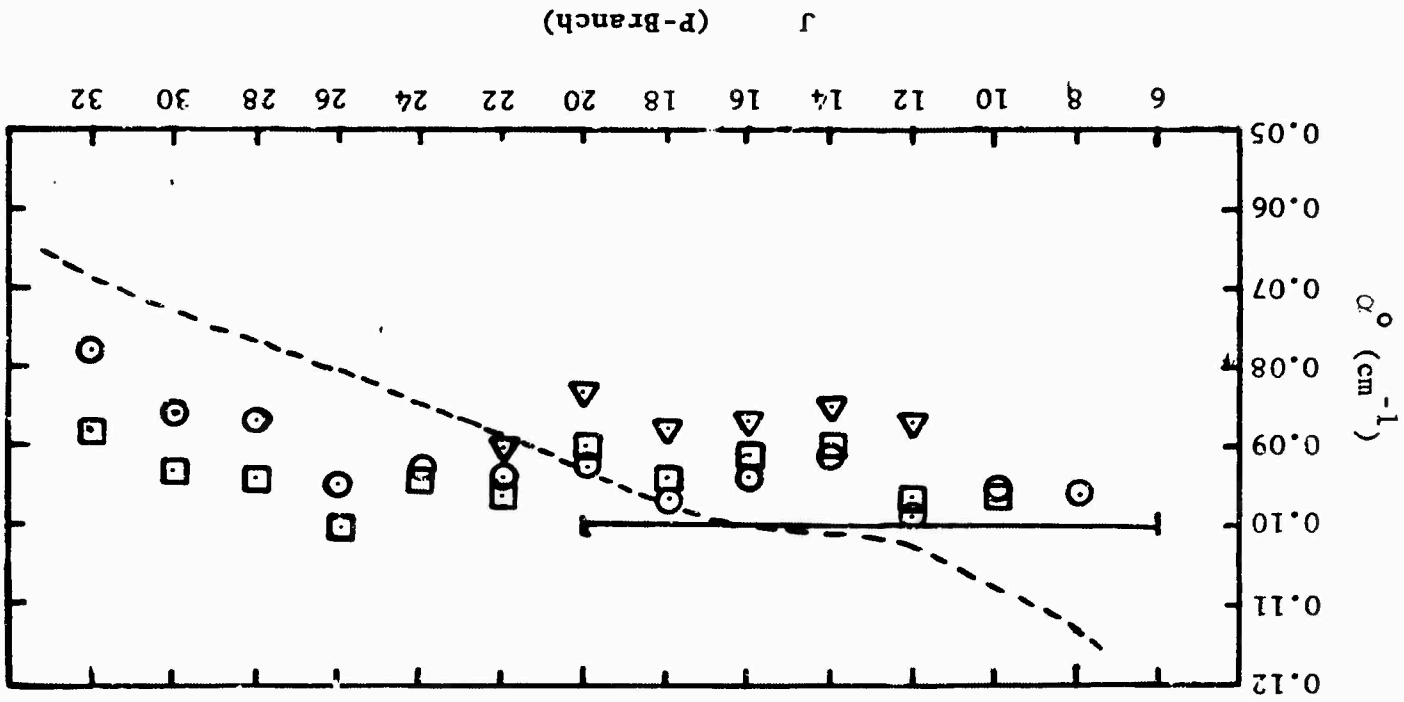
The results of the α^0 measurements are shown by the plotted points in Fig. 3-4; the various geometrical figures correspond to different samples from which the measurement was made. Much of the variation between values for adjacent lines is due to the lines being close together and not completely resolved in the spectra because of the slitwidth of the spectrometer. $\int A(\nu)d\nu$ was calculated between points midway, to the nearest 0.1 cm^{-1} , between line centers. Because of the "rounding-off" of the position of the midpoint and because of slight calibration errors, part of the integral which should be attributed to one line might be attributed to its neighbor.

The solid line represents a mean value of α^0 for lines P6 to P20 in the $O_2^{O_3}$ band which was determined by us.⁸ The dotted curve was obtained from an empirical equation relating α^0 to J which is given by Winters, Silverman and Benedict.¹¹ The equation is based on data in the 15 μ region by Madden.¹⁵

We see that there is reasonably good agreement among the sets of data for J between about 10 and 22. But beyond $J = 22$, the curve based on Winters, Silverman and Benedict drops off quickly while there is only a hint of drop-off in our data. The uncertainty for an average of our points is probably less than 0.01 cm^{-1} .

The various geometrical figures correspond to measurements based on different samples: Δ , 6; \odot , 7, and \square , 9. Solid curve represents mean value for 003 band. Broken curve represents empirical equation by Winters, Silverman and Benedict¹¹ based on 010 band.

FIG. 3-4. HALF-WIDTHS OF SELF-BROADENED CO₂ LINES AT 1 ATM PRESSURE



(This page is intentionally left blank.)

SECTION 4

TABLES OF TRANSMITTANCE

Tables 4-1 and 4-2 consist of values of transmittance, in percent, in the regions 9340 to 9660 cm^{-1} and 8030 to 8340 cm^{-1} , respectively. Values are recorded at intervals of 1 cm^{-1} in Table 4-1 and at intervals of 0.2 cm^{-1} in Table 4-2. In both cases the interval is sufficiently small that the original spectra could be approximated very closely by plotting the tabulated values and joining the points with straight lines. The first and second columns give the wavenumber in vacuum cm^{-1} and the wavelength in microns.

The sample pressure p and absorber thickness u for each sample are shown at the top of the corresponding column. Each sample is designated by the same number as in Table 3-2 and in the spectra shown in Section 3.

Values are not tabulated over some portions of the spectra of the smaller samples where the absorbance is very small. $T(\nu)$ can be considered as 1 ($A(\nu) \approx 0$), for even the largest samples, from 9415 to 9430 cm^{-1} and from 9530 to 9570 cm^{-1} . Several of the spectra from which the tables were obtained, particularly those between 9340 and 9660 cm^{-1} , represent the average of two or three original spectra which were scanned for the same sample. The wavenumber scale was calibrated by using the known positions of the lines indicated in Figures 3-1 and 3-2.

Table 4-1

Item No. P (bars)	3		4		Item No. P (bars)	3		4	
	$V \times 100$	$V \times 100$	$V \times 100$	$V \times 100$		$V \times 100$	$V \times 100$	$V \times 100$	$V \times 100$
9140-C	1.00932	98.9	1.00932	98.9	9140-C	1.00932	98.9	1.00932	98.9
9141-C	1.00930	98.7	1.00930	98.7	9141-C	1.00930	98.7	1.00930	98.7
9142-C	1.00928	98.5	1.00928	98.5	9142-C	1.00928	98.5	1.00928	98.5
9143-C	1.00926	98.3	1.00926	98.3	9143-C	1.00926	98.3	1.00926	98.3
9144-C	1.00924	98.1	1.00924	98.1	9144-C	1.00924	98.1	1.00924	98.1
9145-C	1.00922	97.9	1.00922	97.9	9145-C	1.00922	97.9	1.00922	97.9
9146-C	1.00920	97.7	1.00920	97.7	9146-C	1.00920	97.7	1.00920	97.7
9147-C	1.00918	97.5	1.00918	97.5	9147-C	1.00918	97.5	1.00918	97.5
9148-C	1.00916	97.3	1.00916	97.3	9148-C	1.00916	97.3	1.00916	97.3
9149-C	1.00914	97.1	1.00914	97.1	9149-C	1.00914	97.1	1.00914	97.1
9150-C	1.00912	96.9	1.00912	96.9	9150-C	1.00912	96.9	1.00912	96.9
9151-C	1.00910	96.7	1.00910	96.7	9151-C	1.00910	96.7	1.00910	96.7
9152-C	1.00908	96.5	1.00908	96.5	9152-C	1.00908	96.5	1.00908	96.5
9153-C	1.00906	96.3	1.00906	96.3	9153-C	1.00906	96.3	1.00906	96.3
9154-C	1.00904	96.1	1.00904	96.1	9154-C	1.00904	96.1	1.00904	96.1
9155-C	1.00902	95.9	1.00902	95.9	9155-C	1.00902	95.9	1.00902	95.9
9156-C	1.00900	95.7	1.00900	95.7	9156-C	1.00900	95.7	1.00900	95.7
9157-C	1.00898	95.5	1.00898	95.5	9157-C	1.00898	95.5	1.00898	95.5
9158-C	1.00896	95.3	1.00896	95.3	9158-C	1.00896	95.3	1.00896	95.3
9159-C	1.00894	95.1	1.00894	95.1	9159-C	1.00894	95.1	1.00894	95.1
9160-C	1.00892	94.9	1.00892	94.9	9160-C	1.00892	94.9	1.00892	94.9
9161-C	1.00890	94.7	1.00890	94.7	9161-C	1.00890	94.7	1.00890	94.7
9162-C	1.00888	94.5	1.00888	94.5	9162-C	1.00888	94.5	1.00888	94.5
9163-C	1.00886	94.3	1.00886	94.3	9163-C	1.00886	94.3	1.00886	94.3
9164-C	1.00884	94.1	1.00884	94.1	9164-C	1.00884	94.1	1.00884	94.1
9165-C	1.00882	93.9	1.00882	93.9	9165-C	1.00882	93.9	1.00882	93.9
9166-C	1.00880	93.7	1.00880	93.7	9166-C	1.00880	93.7	1.00880	93.7
9167-C	1.00878	93.5	1.00878	93.5	9167-C	1.00878	93.5	1.00878	93.5
9168-C	1.00876	93.3	1.00876	93.3	9168-C	1.00876	93.3	1.00876	93.3
9169-C	1.00874	93.1	1.00874	93.1	9169-C	1.00874	93.1	1.00874	93.1
9170-C	1.00872	92.9	1.00872	92.9	9170-C	1.00872	92.9	1.00872	92.9
9171-C	1.00870	92.7	1.00870	92.7	9171-C	1.00870	92.7	1.00870	92.7
9172-C	1.00868	92.5	1.00868	92.5	9172-C	1.00868	92.5	1.00868	92.5
9173-C	1.00866	92.3	1.00866	92.3	9173-C	1.00866	92.3	1.00866	92.3
9174-C	1.00864	92.1	1.00864	92.1	9174-C	1.00864	92.1	1.00864	92.1
9175-C	1.00862	91.9	1.00862	91.9	9175-C	1.00862	91.9	1.00862	91.9
9176-C	1.00860	91.7	1.00860	91.7	9176-C	1.00860	91.7	1.00860	91.7
9177-C	1.00858	91.5	1.00858	91.5	9177-C	1.00858	91.5	1.00858	91.5
9178-C	1.00856	91.3	1.00856	91.3	9178-C	1.00856	91.3	1.00856	91.3
9179-C	1.00854	91.1	1.00854	91.1	9179-C	1.00854	91.1	1.00854	91.1
9180-C	1.00852	90.9	1.00852	90.9	9180-C	1.00852	90.9	1.00852	90.9
9181-C	1.00850	90.7	1.00850	90.7	9181-C	1.00850	90.7	1.00850	90.7
9182-C	1.00848	90.5	1.00848	90.5	9182-C	1.00848	90.5	1.00848	90.5
9183-C	1.00846	90.3	1.00846	90.3	9183-C	1.00846	90.3	1.00846	90.3
9184-C	1.00844	90.1	1.00844	90.1	9184-C	1.00844	90.1	1.00844	90.1
9185-C	1.00842	89.9	1.00842	89.9	9185-C	1.00842	89.9	1.00842	89.9
9186-C	1.00840	89.7	1.00840	89.7	9186-C	1.00840	89.7	1.00840	89.7
9187-C	1.00838	89.5	1.00838	89.5	9187-C	1.00838	89.5	1.00838	89.5
9188-C	1.00836	89.3	1.00836	89.3	9188-C	1.00836	89.3	1.00836	89.3
9189-C	1.00834	89.1	1.00834	89.1	9189-C	1.00834	89.1	1.00834	89.1
9190-C	1.00832	88.9	1.00832	88.9	9190-C	1.00832	88.9	1.00832	88.9
9191-C	1.00830	88.7	1.00830	88.7	9191-C	1.00830	88.7	1.00830	88.7
9192-C	1.00828	88.5	1.00828	88.5	9192-C	1.00828	88.5	1.00828	88.5
9193-C	1.00826	88.3	1.00826	88.3	9193-C	1.00826	88.3	1.00826	88.3
9194-C	1.00824	88.1	1.00824	88.1	9194-C	1.00824	88.1	1.00824	88.1
9195-C	1.00822	87.9	1.00822	87.9	9195-C	1.00822	87.9	1.00822	87.9
9196-C	1.00820	87.7	1.00820	87.7	9196-C	1.00820	87.7	1.00820	87.7
9197-C	1.00818	87.5	1.00818	87.5	9197-C	1.00818	87.5	1.00818	87.5
9198-C	1.00816	87.3	1.00816	87.3	9198-C	1.00816	87.3	1.00816	87.3
9199-C	1.00814	87.1	1.00814	87.1	9199-C	1.00814	87.1	1.00814	87.1
9200-C	1.00812	86.9	1.00812	86.9	9200-C	1.00812	86.9	1.00812	86.9

Table 4-2 (continued)

Spec. No. (ft.)	Spec. No. (m)	1	2	3	4	5	6	7	8	9	10	11	12	13	14	15
(m)	(ft.)	0.00 x 10 ⁰	1.00 x 10 ¹	1.00 x 10 ²	1.00 x 10 ³	1.00 x 10 ⁴	1.00 x 10 ⁵	1.00 x 10 ⁶	1.00 x 10 ⁷	1.00 x 10 ⁸	1.00 x 10 ⁹	1.00 x 10 ¹⁰	1.00 x 10 ¹¹	1.00 x 10 ¹²	1.00 x 10 ¹³	1.00 x 10 ¹⁴
8200-0 L-21481	8200-0 L-21481	1.21481	1.21481	1.21481	1.21481	1.21481	1.21481	1.21481	1.21481	1.21481	1.21481	1.21481	1.21481	1.21481	1.21481	1.21481

Table 4-2 (continued)

Sym. No. (plate)	Wavelength (micrometers)															
	1	2	3	4	5	6	7	8	9	10	11	12	13	14	15	16
	1.00	2.00	3.00	4.00	5.00	6.00	7.00	8.00	9.00	10.00	11.00	12.00	13.00	14.00	15.00	16.00
8282.0	1.20344	78.3	62.7	59.1	55.2	52.2	49.4	46.8	44.3	41.9	39.6	37.4	35.2	33.1	31.0	29.0
8282.2	1.20346	78.5	62.9	59.3	55.4	52.4	49.6	47.0	44.5	42.1	39.8	37.6	35.4	33.3	31.2	29.1
8282.4	1.20348	78.7	63.1	59.5	55.6	52.6	49.8	47.2	44.7	42.3	40.0	37.8	35.6	33.5	31.4	29.2
8282.6	1.20350	78.9	63.3	59.7	55.8	52.8	50.0	47.4	44.9	42.5	40.2	38.0	35.8	33.7	31.6	29.4
8282.8	1.20352	79.1	63.5	60.0	56.1	53.1	50.3	47.7	45.1	42.7	40.4	38.2	36.0	33.9	31.8	29.6
8283.0	1.20354	79.3	63.7	60.3	56.4	53.4	50.6	48.0	45.4	43.0	40.7	38.5	36.3	34.2	32.1	29.9
8283.2	1.20356	79.5	63.9	60.6	56.7	53.7	50.9	48.3	45.7	43.3	41.0	38.8	36.6	34.5	32.4	30.2
8283.4	1.20358	79.7	64.1	60.9	57.0	54.0	51.2	48.6	46.0	43.6	41.3	39.1	36.9	34.8	32.7	30.5
8283.6	1.20360	79.9	64.3	61.2	57.3	54.3	51.5	48.9	46.3	43.9	41.6	39.4	37.2	35.1	33.0	30.8
8283.8	1.20362	80.1	64.5	61.5	57.6	54.6	51.8	49.2	46.6	44.2	41.9	39.7	37.5	35.4	33.3	31.1
8284.0	1.20364	80.3	64.7	61.8	57.9	54.9	52.1	49.5	46.9	44.5	42.2	40.0	37.8	35.7	33.6	31.4
8284.2	1.20366	80.5	64.9	62.1	58.2	55.2	52.4	49.8	47.2	44.8	42.5	40.3	38.1	36.0	33.9	31.7
8284.4	1.20368	80.7	65.1	62.4	58.5	55.5	52.7	50.1	47.5	45.1	42.8	40.6	38.4	36.3	34.2	32.0
8284.6	1.20370	80.9	65.3	62.7	58.8	55.8	53.0	50.4	47.8	45.4	43.1	40.9	38.7	36.6	34.5	32.3
8284.8	1.20372	81.1	65.5	63.0	59.1	56.1	53.3	50.7	48.1	45.7	43.4	41.2	39.0	36.9	34.8	32.6
8285.0	1.20374	81.3	65.7	63.3	59.4	56.4	53.6	51.0	48.4	46.0	43.7	41.5	39.3	37.2	35.1	32.9
8285.2	1.20376	81.5	65.9	63.6	59.7	56.7	53.9	51.3	48.7	46.3	44.0	41.8	39.6	37.5	35.4	33.2
8285.4	1.20378	81.7	66.1	63.9	60.0	57.0	54.2	51.6	49.0	46.6	44.3	42.1	39.9	37.8	35.7	33.5
8285.6	1.20380	81.9	66.3	64.2	60.3	57.3	54.5	51.9	49.3	46.9	44.6	42.4	40.2	38.1	36.0	33.8
8285.8	1.20382	82.1	66.5	64.5	60.6	57.6	54.8	52.2	49.6	47.2	44.9	42.7	40.5	38.4	36.3	34.1
8286.0	1.20384	82.3	66.7	64.8	60.9	57.9	55.1	52.5	49.9	47.5	45.2	43.0	40.8	38.7	36.6	34.4
8286.2	1.20386	82.5	66.9	65.1	61.2	58.2	55.4	52.8	50.2	47.8	45.5	43.3	41.1	39.0	36.9	34.7
8286.4	1.20388	82.7	67.1	65.4	61.5	58.5	55.7	53.1	50.5	48.1	45.8	43.6	41.4	39.3	37.2	35.0
8286.6	1.20390	82.9	67.3	65.7	61.8	58.8	56.0	53.4	50.8	48.4	46.1	43.9	41.7	39.6	37.5	35.3
8286.8	1.20392	83.1	67.5	66.0	62.1	59.1	56.3	53.7	51.1	48.7	46.4	44.2	42.0	39.9	37.8	35.6
8287.0	1.20394	83.3	67.7	66.3	62.4	59.4	56.6	54.0	51.4	49.0	46.7	44.5	42.3	40.2	38.1	35.9
8287.2	1.20396	83.5	67.9	66.6	62.7	59.7	56.9	54.3	51.7	49.3	47.0	44.8	42.6	40.5	38.4	36.2
8287.4	1.20398	83.7	68.1	66.9	63.0	60.0	57.2	54.6	52.0	49.6	47.3	45.1	42.9	40.8	38.7	36.5
8287.6	1.20400	83.9	68.3	67.2	63.3	60.3	57.5	54.9	52.3	49.9	47.6	45.4	43.2	41.1	39.0	36.8
8287.8	1.20402	84.1	68.5	67.5	63.6	60.6	57.8	55.2	52.6	50.2	47.9	45.7	43.5	41.4	39.3	37.1
8288.0	1.20404	84.3	68.7	67.8	63.9	60.9	58.1	55.5	52.9	50.5	48.2	46.0	43.8	41.7	39.6	37.4
8288.2	1.20406	84.5	68.9	68.1	64.2	61.2	58.4	55.8	53.2	50.8	48.5	46.3	44.1	42.0	39.9	37.7
8288.4	1.20408	84.7	69.1	68.4	64.5	61.5	58.7	56.1	53.5	51.1	48.8	46.6	44.4	42.3	40.2	38.0
8288.6	1.20410	84.9	69.3	68.7	64.8	61.8	59.0	56.4	53.8	51.4	49.1	46.9	44.7	42.6	40.5	38.3
8288.8	1.20412	85.1	69.5	69.0	65.1	62.1	59.3	56.7	54.1	51.7	49.4	47.2	45.0	42.9	40.8	38.6
8289.0	1.20414	85.3	69.7	69.3	65.4	62.4	59.6	57.0	54.4	52.0	49.7	47.5	45.3	43.2	41.1	38.9
8289.2	1.20416	85.5	69.9	69.6	65.7	62.7	59.9	57.3	54.7	52.3	50.0	47.8	45.6	43.5	41.4	39.2
8289.4	1.20418	85.7	70.1	69.9	66.0	63.0	60.2	57.6	55.0	52.6	50.3	48.1	45.9	43.8	41.7	39.5
8289.6	1.20420	85.9	70.3	70.2	66.3	63.3	60.5	57.9	55.3	52.9	50.6	48.4	46.2	44.1	42.0	39.8
8289.8	1.20422	86.1	70.5	70.5	66.6	63.6	60.8	58.2	55.6	53.2	50.9	48.7	46.5	44.4	42.3	40.1
8290.0	1.20424	86.3	70.7	70.8	66.9	63.9	61.1	58.5	55.9	53.5	51.2	49.0	46.8	44.7	42.6	40.4
8290.2	1.20426	86.5	70.9	71.1	67.2	64.2	61.4	58.8	56.2	53.8	51.5	49.3	47.1	45.0	42.9	40.7
8290.4	1.20428	86.7	71.1	71.4	67.5	64.5	61.7	59.1	56.5	54.1	51.8	49.6	47.4	45.3	43.2	41.0
8290.6	1.20430	86.9	71.3	71.7	67.8	64.8	62.0	59.4	56.8	54.4	52.1	49.9	47.7	45.6	43.5	41.3
8290.8	1.20432	87.1	71.5	72.0	68.1	65.1	62.3	59.7	57.1	54.7	52.4	50.2	48.0	45.9	43.8	41.6
8291.0	1.20434	87.3	71.7	72.3	68.4	65.4	62.6	60.0	57.4	55.0	52.7	50.5	48.3	46.2	44.1	41.9
8291.2	1.20436	87.5	71.9	72.6	68.7	65.7	62.9	60.3	57.7	55.3	53.0	50.8	48.6	46.5	44.4	42.2
8291.4	1.20438	87.7	72.1	72.9	69.0	66.0	63.2	60.6	58.0	55.6	53.3	51.1	48.9	46.8	44.7	42.5
8291.6	1.20440	87.9	72.3	73.2	69.3	66.3	63.5	60.9	58.3	55.9	53.6	51.4	49.2	47.1	45.0	42.8
8291.8	1.20442	88.1	72.5	73.5	69.6	66.6	63.8	61.2	58.6	56.2	53.9	51.7	49.5	47.4	45.3	43.1
8292.0	1.20444	88.3	72.7	73.8	69.9	66.9	64.1	61.5	58.9	56.5	54.2	52.0	49.8	47.7	45.6	43.4
8292.2	1.20446	88.5	72.9	74.1	70.2	67.2	64.4	61.8	59.2	56.8	54.5	52.3	50.1	48.0	45.9	43.7
8292.4	1.20448	88.7	73.1	74.4	70.5	67.5	64.7	62.1	59.5	57.1	54.8	52.6	50.4	48.3	46.2	44.0
8292.6	1.20450	88.9	73.3	74.7	70.8	67.8	65.0	62.4	59.8	57.4	55.1	52.9	50.7	48.6	46.5	44.3
8292.8	1.20452	89.1	73.5	75.0	71.1	68.1	65.3	62.7	60.1	57.7	55.4	53.2	51.0	48.9	46.8	44.6
8293.0	1.20454	89.3	73.7	75.3	71.4	68.4	65.6	63.0	60.4	58.0	55.7	53.5	51.3	49.2	47.1	44.9
8293.2	1.20456	89.5	73.9	75.6	71.7	68.7	65.9	63.3	60.7	58.3	56.0	53.8	51.6	49.5	47.4	45.2
8293.4	1.20458	89.7	74.1	75.9	72.0	69.0	66.2	63.6	61.0	58.6	56.3	54.1	51.9	49.8	47.7	45.5
8293.6	1.20460	89.9	74.3	76.2	72.3	69.3	66.5	63.9	61.3	58.9	56.6	54.4	52.2	50.1	48.0	45.8
8293.8	1.20462	90.1	74.5	76.5	72.6	69.6	66.8	64.2	61.6	59.2	56.9	54.7	52.5	50.4	48.3	46.1
8294.0	1.20464	90.3	74.7	76.8	72.9	69.9	67.1	64.5	61.9	59.5	57.2	55.0	52.8	50.7	48.6	46.4
8294.2	1.20466	90.5	74.9	77.1	73.2	70.2	67.4	64.8	62.2	59.8	57.5	55.3	53.1	51.0	48.9	46.7
8294.4	1.20468	90.7	75.1	77.4	73.5	70.5	67.7	65.1	62.5	60.1	57.8	55.6	53.4	51.3	49.2	47.0
8294.6	1.20470	90.9	75.3	77.7	73.8	70.8	68.0	65.4	62.8	60.4	58.1	55.9	53.7	51.6	49.5	47.3
8294.8	1.20472	91.1	75.5	78.0	74.1	71.1	68.3	65.7	63.1	60.7	58.4	56.2	54.0	51.9	49.8	47.6
8295.0	1.20474	91.3	75.7	78.3	74.4	71.4	68.6	66.0	63.4	61.0	58.7	56.5	54.3	52.2	50.1	47.9
8295.2	1.20476	91.5	75.9	78.6	74.7	71.7	68.9	66.3	63.7	61.3	59.0	56.8	54.6	52.5	50.4	48.2
8295.4	1.20478	91.7	76.1	78.9	75.0	72.0	69.2	66.6	64.0	61.6	59.3	57.1	54.9	52.8	50.7	48.5
8295.6	1.20480	91.9	76.3	79.2	75.3	72.3	69.5	66.9	64.3	61.9	59.6	57.4	55.2	53.1	51.0	48.8
8295.8	1.20482	92.1	76.5	79.5	75.6	72.6	69.8	67.2	64.6	62.2	60.0	57.7	55.5	53.4	51.3	49.1
8296.0	1.20484	92.3	76.7	79.8	75.9	72.9	70.1	67.5	64.9	62.5	60.3	58.0	55.8	53.7	51.6	49.4
8296.2	1.20486	92.5	76.9	80.1	76.2	73.2	70.4	67.8	65.2	62.8	60.6	58.3	56.1	54.0	51.9	49.7
8296.4	1.20488	92.7	77.1	80.4	76.5	73.5	70.7	68.1	65.5	63.1	60.9	58.6	56.4	54.3	52.2	50.0
8296.6	1.20490	92.9	77.3	80.7	76.8	73.8	71.0	68.4								

SECTION 5

TABLES OF INTEGRATED ABSORPTIANCE

Values of the integrated absorbance are presented in Tables 5-1 and 5-2 for the 9430-9660 cm^{-1} and 8030-8340 cm^{-1} intervals, respectively. The integrals were calculated from the transmittance tables in Section 4 by assuming that the spectrum could be constructed by plotting the transmittance values and joining them with straight lines.

The lower limit of integration ν' , which is shown at the top of each column, was chosen at a point where there was essentially no absorption. The integrated absorbance between any two wavenumbers listed can be found by subtracting the values tabulated at those two points. Values are tabulated at intervals of 5 cm^{-1} in Table 5-1 which covers samples whose spectra have but little structure. Table 5-2 includes samples whose spectra have considerable structure. Throughout most of the region, the integral is tabulated at points midway between the absorption lines. In regions where the spectra are smooth, tabulations are made at intervals of 5 or 10 cm^{-1} .

Table 5-1 $\left[\int_0^{\infty} A(\nu) d\nu \right]$

Sam. No.	P (atm)	u (atm cm)	ν (cm ⁻¹)
4	2.50 x 10 ³	2.17 x 10 ³	ν = 9570 cm ⁻¹
3	2.50 x 10 ³	1.63 x 10 ³	ν = 9570 cm ⁻¹
2	2.50 x 10 ³	1.09 x 10 ³	ν = 9570 cm ⁻¹
4	2.50 x 10 ³	2.17 x 10 ³	ν = 9430 cm ⁻¹
3	2.50 x 10 ³	1.63 x 10 ³	ν = 9430 cm ⁻¹
2	2.50 x 10 ³	1.09 x 10 ³	ν = 9430 cm ⁻¹
1	2.50 x 10 ³	5.51 x 10 ³	ν = 9430 cm ⁻¹
4	2.50 x 10 ³	2.17 x 10 ³	ν = 9360 cm ⁻¹
3	2.50 x 10 ³	1.63 x 10 ³	ν = 9360 cm ⁻¹
2	2.50 x 10 ³	1.09 x 10 ³	ν = 9360 cm ⁻¹

5-2

Table 5-2 $\int A(v)dv$

Atom, Ion, (eV/cm)	5	6	7	8	9	10	11	12	13	14
v (cm ⁻¹)	$v \cdot 10^{-3}$	$v \cdot 10^{-3}$	$v \cdot 10^{-3}$	$v \cdot 10^{-3}$	$v \cdot 10^{-3}$	$v \cdot 10^{-3}$	$v \cdot 10^{-3}$	$v \cdot 10^{-3}$	$v \cdot 10^{-3}$	$v \cdot 10^{-3}$
8130.0	0	0	0	0	0	0	0	0	0	0
8140.0	0	0	0	0	0	0	0	0	0	0
8150.0	0	0	0	0	0	0	0	0	0	0
8160.0	0	0	0	0	0	0	0	0	0	0
8170.0	0	0	0	0	0	0	0	0	0	0
8180.0	0	0	0	0	0	0	0	0	0	0
8190.0	0	0	0	0	0	0	0	0	0	0
8200.0	0	0	0	0	0	0	0	0	0	0
8210.0	0	0	0	0	0	0	0	0	0	0
8220.0	0	0	0	0	0	0	0	0	0	0
8230.0	0	0	0	0	0	0	0	0	0	0
8240.0	0	0	0	0	0	0	0	0	0	0
8250.0	0	0	0	0	0	0	0	0	0	0
8260.0	0	0	0	0	0	0	0	0	0	0
8270.0	0	0	0	0	0	0	0	0	0	0
8280.0	0	0	0	0	0	0	0	0	0	0
8290.0	0	0	0	0	0	0	0	0	0	0
8300.0	0	0	0	0	0	0	0	0	0	0
8310.0	0	0	0	0	0	0	0	0	0	0
8320.0	0	0	0	0	0	0	0	0	0	0
8330.0	0	0	0	0	0	0	0	0	0	0
8340.0	0	0	0	0	0	0	0	0	0	0
8350.0	0	0	0	0	0	0	0	0	0	0
8360.0	0	0	0	0	0	0	0	0	0	0
8370.0	0	0	0	0	0	0	0	0	0	0
8380.0	0	0	0	0	0	0	0	0	0	0
8390.0	0	0	0	0	0	0	0	0	0	0
8400.0	0	0	0	0	0	0	0	0	0	0
8410.0	0	0	0	0	0	0	0	0	0	0
8420.0	0	0	0	0	0	0	0	0	0	0
8430.0	0	0	0	0	0	0	0	0	0	0
8440.0	0	0	0	0	0	0	0	0	0	0
8450.0	0	0	0	0	0	0	0	0	0	0
8460.0	0	0	0	0	0	0	0	0	0	0
8470.0	0	0	0	0	0	0	0	0	0	0
8480.0	0	0	0	0	0	0	0	0	0	0
8490.0	0	0	0	0	0	0	0	0	0	0
8500.0	0	0	0	0	0	0	0	0	0	0
8510.0	0	0	0	0	0	0	0	0	0	0
8520.0	0	0	0	0	0	0	0	0	0	0
8530.0	0	0	0	0	0	0	0	0	0	0
8540.0	0	0	0	0	0	0	0	0	0	0
8550.0	0	0	0	0	0	0	0	0	0	0
8560.0	0	0	0	0	0	0	0	0	0	0
8570.0	0	0	0	0	0	0	0	0	0	0
8580.0	0	0	0	0	0	0	0	0	0	0
8590.0	0	0	0	0	0	0	0	0	0	0
8600.0	0	0	0	0	0	0	0	0	0	0
8610.0	0	0	0	0	0	0	0	0	0	0
8620.0	0	0	0	0	0	0	0	0	0	0
8630.0	0	0	0	0	0	0	0	0	0	0
8640.0	0	0	0	0	0	0	0	0	0	0
8650.0	0	0	0	0	0	0	0	0	0	0
8660.0	0	0	0	0	0	0	0	0	0	0
8670.0	0	0	0	0	0	0	0	0	0	0
8680.0	0	0	0	0	0	0	0	0	0	0
8690.0	0	0	0	0	0	0	0	0	0	0
8700.0	0	0	0	0	0	0	0	0	0	0
8710.0	0	0	0	0	0	0	0	0	0	0
8720.0	0	0	0	0	0	0	0	0	0	0
8730.0	0	0	0	0	0	0	0	0	0	0
8740.0	0	0	0	0	0	0	0	0	0	0
8750.0	0	0	0	0	0	0	0	0	0	0
8760.0	0	0	0	0	0	0	0	0	0	0
8770.0	0	0	0	0	0	0	0	0	0	0
8780.0	0	0	0	0	0	0	0	0	0	0
8790.0	0	0	0	0	0	0	0	0	0	0
8800.0	0	0	0	0	0	0	0	0	0	0
8810.0	0	0	0	0	0	0	0	0	0	0
8820.0	0	0	0	0	0	0	0	0	0	0
8830.0	0	0	0	0	0	0	0	0	0	0
8840.0	0	0	0	0	0	0	0	0	0	0
8850.0	0	0	0	0	0	0	0	0	0	0
8860.0	0	0	0	0	0	0	0	0	0	0
8870.0	0	0	0	0	0	0	0	0	0	0
8880.0	0	0	0	0	0	0	0	0	0	0
8890.0	0	0	0	0	0	0	0	0	0	0
8900.0	0	0	0	0	0	0	0	0	0	0
8910.0	0	0	0	0	0	0	0	0	0	0
8920.0	0	0	0	0	0	0	0	0	0	0
8930.0	0	0	0	0	0	0	0	0	0	0
8940.0	0	0	0	0	0	0	0	0	0	0
8950.0	0	0	0	0	0	0	0	0	0	0
8960.0	0	0	0	0	0	0	0	0	0	0
8970.0	0	0	0	0	0	0	0	0	0	0
8980.0	0	0	0	0	0	0	0	0	0	0
8990.0	0	0	0	0	0	0	0	0	0	0
9000.0	0	0	0	0	0	0	0	0	0	0

(This page is left intentionally blank.)

SECTION 6

REFERENCES

1. G. Herzberg and L. Herzberg, J. Opt. Soc. Am. 43, 1037 (1953).
2. D. E. Burch, D. A. Gryvnak and R. R. Patty, Absorption of CO₂ Between 4500 and 5400 cm⁻¹, Aeronutronic Report U-2955, Contract N0nr 3560(00), (15 December 1964).
3. D. E. Burch, R. R. Patty and D. A. Gryvnak, Absorption and Emission of Infrared Radiation by CO₂ and H₂O, Aeronutronic Report U-2367, Contract N0nr 3560(00), (26 November 1963).
4. D. E. Burch, D. A. Gryvnak and Dudley Williams, Appl. Opt. 1, 759, (1962).
5. D. E. Burch, D. A. Gryvnak, R. R. Patty and Charlotte Bartky, The Shapes of Collision-Broadened CO₂ Absorption Lines, Aeronutronic Report U-3203, Contract N0nr 3560(00), (1965).
6. C. P. Courtoy, Annales de la Societe Scientifique de Bruxelles, Serie 1, pp 5-230 (27 March 1959). Also, C. P. Courtoy, Canad. J. Phys. 35, 608 (1957).
7. V. R. Stull, P. J. Wyatt and G. N. Plass, The Infrared Absorption of Carbon Dioxide, Aeronutronic Report U-1505, Contract AF 19(604)-7479, (30 December 1961).
8. D. E. Burch, D. A. Gryvnak and R. R. Patty, Absorption by CO₂ Between 6600 and 7125 cm⁻¹ (1.4 Micron Region), Aeronutronic Report U-3127, Contract N0nr 3560(00), (1965).
9. L. D. Gray and J. E. Selvidge, J. Quant. Spectros. Radiat. Transfer 5, 291, (1965).
10. G. Herzberg, Infrared and Raman Spectra of Polyatomic Molecules, D. Van Nostrand Co. (See 266 ff for a discussion of the intensities of difference bands) (Ninth printing 1960).

REFERENCES

(Continued)

11. B. H. Winters, S. Silverman and W. S. Benedict, J. Quant. Spec. 4, 527 (1964).
12. R. Ladenberg and F. Reiche, Ann. Physik 42, 181 (1913).
13. L. D. Kaplan and D. F. Eggers, Jr., J. Chem. Phys. 25, 876 (1956).
14. G. N. Plass, J. Opt. Soc. Am. 55, 104 (1965).
15. R. P. Madden, J. Chem. Phys 35, No. 6, 2083 (1961).